Antiviral Research 93 (2012) 30–38

Contents lists available at SciVerse ScienceDirect

Antiviral Research

journal homepage: www.elsevier.com/locate/antiviral

Identification of a novel resistance mutation for benzimidazole inhibitors of the HCV RNA-dependent RNA polymerase

Leen Delang [a], Mathy Froeyen [b], Piet Herdewijn [b], Johan Neyts [a,*]

[a] Department of Microbiology and Immunology, Rega Institute for Medical Research, K.U.Leuven, Belgium
[b] Laboratory for Medicinal Chemistry, Rega Institute for Medical Research, K.U.Leuven, Belgium

ARTICLE INFO

Article history:
Received 29 July 2011
Revised 4 October 2011
Accepted 11 October 2011
Available online 19 October 2011

Keywords:
Hepatitis C virus
Non-nucleoside polymerase inhibitor
Benzimidazole
Resistance

ABSTRACT

Non-nucleoside inhibitors of the RNA-dependent RNA polymerase of the hepatitis C virus that are based on a benzimidazole or indole scaffold have been reported to interact with thumb domain 1 of the enzyme. Escape mutants that confer *in vitro* resistance to these inhibitors map to amino acids P495, P496 or V499. We here report a novel resistance mutation (T389S/A) that was identified following resistance selection with the benzimidazole non-nucleoside polymerase inhibitor JT-16 in HCV Con-1 subgenomic replicon (genotype 1b). This JT-16 resistant replicon retained wild-type susceptibility to protease inhibitors and nucleoside polymerase inhibitors. Replicons that carry mutations T389A and T389S have moderate levels of resistance to JT-16 (7- and 13-fold, respectively). Mutation P495A is associated with high-level (44-fold) resistance. Surprisingly, this previously reported 'key' mutation for benzimidazole resistance, P495A, was detected in only 15% of the resistant population. Furthermore, the replication fitness of the T389S mutant was significantly higher than that of the P495A mutant. By means of molecular modeling a structural hypothesis was formulated to explain the emergence of the T389S/A mutation in the JT-16 resistant replicon. Our data demonstrate that low-level resistant, but fit, variants can develop during *in vitro* resistance selection with the benzimidazole inhibitor JT-16. Moreover, different substitutions to the benzimidazole scaffold can affect the (pattern of) resistance mutations that emerge during resistance selection.

© 2011 Elsevier B.V. All rights reserved.

1. Introduction

Hepatitis C virus (HCV) is a single-stranded (+)-RNA virus belonging to the family of the *Flaviviridae*. Worldwide, 170 million people are chronically infected with HCV (Shepard et al., 2005). Chronic HCV infection can evolve to cirrhosis and hepatocellular carcinoma. In developed countries, HCV infection is the major reason for liver transplantation. The current standard of care consists of the combination of pegylated interferon (IFN) and ribavirin (Zeuzem et al., 2009). Unfortunately, standard of care is associated with severe adverse effects and low efficacy, in particular in genotype 1 HCV-infected patients. Therefore, more selective, potent and safe HCV inhibitors are being or have recently been developed (Delang et al., 2010).

The RNA-dependent RNA polymerase (NS5B) of HCV is essential for viral RNA replication and is thus an excellent target for inhibition of viral replication. The HCV NS5B catalyses the synthesis of a complementary minus-strand RNA using the (incoming) RNA genome as a template and subsequently the synthesis of new progeny genomic plus-strand RNA from the minus-strand RNA template. The three-dimensional structure is similar to that of other polymerases and is often compared with a right hand (Bressanelli et al., 1999). The palm domain contains the catalytic site and the fingers and the thumb domain are responsible for the interaction with the RNA. Similar to other RNA-dependent RNA polymerases are the two finger loops that extend from the finger domain and that make contact with the thumb domain, resulting in an encircled active site. A distinct feature of the HCV polymerase is the protrusion of a β–hairpin from the thumb domain into the active site (Hong et al., 2001). This β–hairpin is involved in the initiation of *de novo* RNA synthesis. Furthermore, a C-terminal region folds from the surface of the thumb domain towards the active site, probably involved in template selection (Leveque et al., 2003). At the interface of the finger and thumb domain, a GTP-binding site was identified on the polymerase surface, 30 Å away from the catalytic site. This GTP pocket was proposed to be a potential allosteric regulatory site that could modulate interactions between these two domains during the conformational change needed for efficient initiation (Bressanelli et al., 2002).

Both nucleoside (NI) and non-nucleoside (NNI) polymerase inhibitors are in preclinical and clinical development. Nucleoside polymerase inhibitors (NI) act as virtual chain terminators. In this

* Corresponding author. Address: Rega Institute for Medical Research, Minderbroedersstraat 10, B-3000 Leuven, Belgium. Tel.: +32 16337341; fax: +32 16337340.
E-mail address: Johan.Neyts@rega.kuleuven.be (J. Neyts).

0166-3542/$ - see front matter © 2011 Elsevier B.V. All rights reserved.
doi:10.1016/j.antiviral.2011.10.012

class of inhibitors, R7128, a prodrug of β-D-2′-deoxy-2′-fluoro-2′-C-methylcytidine is the most advanced. Non-nucleoside polymerase inhibitors (NNI) act as allosteric inhibitors and are non-competitive with nucleotide triphosphates. They inhibit the catalytic efficiency of the enzyme's active site machinery by preventing a conformational transition needed for the initiation of RNA synthesis. Their binding sites are located outside the catalytic site of the polymerase. Four different allosteric sites are identified: (i) thumb domain 1 (site A), (ii) thumb domain 2 (site B), (iii) palm domain 1 (site C) and (iv) palm domain 2 (site D). Thumb domain 1 is located at the junction of the thumb domain and the N-terminal λ1 loop (Kukolj et al., 2005). Benzimidazole and indole derived structures can inhibit HCV replication by interacting with thumb domain 1. Thiophene carboxylic acid, dihydropyranones and pyranoindoles were identified to target thumb domain 2, a hydrophobic cavity located at the base of the thumb domain. Palm domain 1 and 2 are overlapping regions located at the junction of the palm and thumb domain in close proximity of the catalytic site. NNIs that bind to palm domain 1 are benzothiadiazines and acylpyrrolidines. Benzofuran-based inhibitors bind to palm domain 2 (Delang et al., 2010).

The first benzimidazole inhibitors were identified by high-throughput screening at Boehringer Ingelheim and Japan Tobacco. The *in vitro* antiviral efficacy of benzimidazole inhibitors was previously demonstrated in HCV subgenomic replicons (Kukolj et al., 2005; Tomei et al., 2003). A 1,2-disubstituted benzimidazole-5-carboxylic acid scaffold was identified as the minimum core for biological activity. Benzimidazole analog JTK-003 (Japan Tobacco) was studied in early clinical trials, but development was halted for unknown reasons. Unlike Japan Tobacco that concentrated on optimization of the right-hand side of the benzimidazole scaffold, Boehringer Ingelheim elaborated on the left-hand side of the scaffold through formation of amide derivatives. Further optimization of the cellular permeability by conversion of the benzimidazole scaffold to the more lipophilic indole scaffold provided further enhancement of antiviral activity (Beaulieu et al., 2006). Such indole-based inhibitors (BILB 1941, BI 207127, MK-3281) have been investigated in clinical phase I trials (Erhardt et al., 2009; Brainard et al., 2009). BI 207127 is currently in phase II of clinical development. In phase I trials, patients infected with genotype 1 HCV were treated with BI 207127 for 5 days as mono-therapy. The antiviral activity of BI 207127 reached a maximal effect (median 3.8 $\log_{10}$ decline in viral load) for the group receiving 800 mg q8h. BI 207127 resistant variants were observed in 11% of patients who received 5-day mono-therapy (Larrey et al., 2009).

The enzyme-bound conformation of a benzimidazole inhibitor, as determined by NMR experiments, suggests that indole- and benzimidazole-based inhibitors bind to the same allosteric binding site (LaPlante et al., 2004). This binding site was elucidated by Di Marco and colleagues (Di Marco et al., 2005). Crystal structures of HCV NS5B with an indole-based inhibitor showed that this inhibitor binds to a site on the surface of the thumb domain, located at the junction of the thumb domain and the N-terminal λ1 loop. Interestingly, in the apoenzyme, this binding site is occupied by a small α-helix of the λ1 fingertip loop that connects the fingers and the thumb domains. Indole and benzimidazole inhibitors may therefore inhibit HCV NS5B by preventing the formation of intramolecular contacts between these two domains. Comparison of the NS5B-GTP structure and the NS5B-indole structure showed that the binding sites for GTP and for the indole-based inhibitors are close in space but clearly distinct. *In vitro* resistance studies with HCV subgenomic replicons revealed that resistance mutations to benzimidazole inhibitors emerged at amino acid positions P495, P496 or V499 (Tomei et al., 2003; Kukolj et al., 2005). Both P495 and P496 are strictly conserved across all HCV genotypes. Interestingly, P495 is part of the GTP binding pocket at the interface between the finger and thumb domains. It was shown that increasing GTP concentrations resulted in increased IC_{50} values of benzimidazole inhibitors, demonstrating that GTP interferes with the inhibition by these compounds (Tomei et al., 2003). Despite the conservation of P495 across HCV genotypes, thumb domain 1 inhibitors are significantly less active on enzymes and replicons derived from genotype 2 clinical isolates (Rydberg et al., 2009; Herlihy et al., 2008). A genotypic variant in genotype 2 at position 392 (L392I) has been shown to result in a different shape of the binding pocket of thumb domain 1 and is thereby partly responsible for the resistance of the genotype 2 polymerase to this class of inhibitors (Rydberg et al., 2009).

In this study, we report a novel resistance mutation (T389S/A) that was identified following resistance selection with the benzimidazole inhibitor JT-16 in HCV Con-1 subgenomic replicon. Site-directed mutagenesis was performed to elucidate the contribution of this mutation to JT-16 resistance. Also, the replication fitness of these new mutants and of previously reported resistant mutants (P495A, P496S) was studied. Furthermore, by means of molecular modeling a structural hypothesis was formulated to explain the emergence of the T389S/A mutation in the JT-16 resistant replicon.

2. Materials and methods

2.1. HCV replicon

Huh-7 cells containing subgenomic HCV replicon I_{377}/NS3-3′/wt (Huh 9-13) have been described before (Lohmann et al., 1999). Cells were cultured in Dulbecco's modified Eagle's Medium (DMEM; Gibco) supplemented with 10% heat-inactivated fetal bovine serum (Integro), 1× non-essential amino acids, 100 IU/ml penicillin (Gibco), 100 μg/ml streptomycin (Gibco), 1 mg/ml Geneticin® (G418; Gibco). Cell cultures were maintained at 37 °C in an atmosphere of 5% CO_2. Huh-Lunet cells, which are derived from a cell clone that was generated by "curing" Huh-7 replicon cells with a selective drug, were cultured without G418 (Friebe et al., 2005).

2.2. HCV inhibitors

Benzimidazole inhibitor JT-16 ([2-[4-[[4-(acetylamino)-4′-chloro-[1,1′-biphenyl]-2-yl]methoxy] phenyl]-1-cyclohexyl-1H-benzimidazole-5-carboxylic acid) was synthesized as described previously (Hashimoto, 2005). HCV reference inhibitors benzofuran HCV-796, thiophene carboxylic acid, benzothiadiazine GSK-4, 2′-C-methylcytidine and VX-950 were synthesized as described before (Paeshuyse et al., 2008).

2.3. Resistance selection

Approximately 3×10^5 Huh 9-13 replicon-containing cells were seeded in a T25 tissue culture flask in complete DMEM with G418 and under constant antiviral pressure of benzimidazole JT-16 (1× EC_{50}). The cells were subcultured when 80% confluence was reached. Following three passages at 1× EC_{50}, Huh 9-13 cells were challenged with increasing doses of antiviral pressure until the highest non-cytotoxic concentration was reached. When replicon-containing cells suffered from compound pressure (as a result of a too low level of replicon content), G418 and compound pressure were removed till cells recovered.

2.4. Antiviral assays

Antiviral assays were performed as described before (Delang et al., 2009). Briefly, cells were seeded at a density of 5×10^3 cells

per well in a 96-well cell culture plate in complete DMEM. Following incubation for 24 h at 37 °C (5% CO_2), serial dilutions of the test compounds in complete DMEM were added in a total volume of 100 μl. HCV replicon RNA levels were determined by a reverse transcription quantitative polymerase chain reaction (RT-qPCR). Primers used for detection of HCV replicon RNA were: 5′-CCG GCT ACC TGC CCA TTC-3′ (forward primer), 5′-CCA GAT CAT CCT GAT CGA CAA G-3′ (reverse primer) and 5′-FAM-ACA TCG CAT CGA GCG AGC ACG TAC-TAMRA-3′ (probe).

2.5. Site-directed mutagenesis

Initially, the NS5B gene was excised from the pFK I389 Lucubineo EI NS3-3′ET construct by SpeI–XhoI restriction digestion and subcloned to construct pCRII-HCV5B. Mutations were introduced into pCRII-HCV5B by using the Quickchange® Site-Directed Mutagenesis Kit (Agilent, Stratagene Products). Following primers were used: 5′-CCGT GACCCCGCCACCCCCCTTG-3′ (T389A-forward), 5′-CA AGGGGGGTGGCGGGGTCACGG -3′ (T389A-reverse), 5′-CACCCGTG ACCCCTCCACCCCCCTTG-3′ (T389S-forward), 5′-CAA GGGGGGTGG AGGGGTCACGGGTG-3′ (T389S-reverse), 5′-GGAAACTTGGGGTAG CG CCCTTGCGAGTCTGG-3′ (P495A-forward), 5′-CCAGACTCGCAA GGGCGCTACCCCAAG TTTCC-3′(P495A-reverse), 5′-CTTGGGGTACC GTCCTTGCGAGTCTGG-3′ (P496S-forward), 5′-CCAGACTCGCAAG-GACGGTACCCCAAG-3′ (P496S-reverse). The 50 μl reaction mixture contained 1× reaction buffer, 50 ng plasmid, 125 ng forward primer, 125 ng reverse primer, 1 μl dNTP mix and 2.5 U PfuTurbo DNA polymerase. Thermal cycling was performed as follows: denaturation at 95 °C 30 s, followed by 12 cycles of 30 s at 95 °C, 1 min at 55 °C and 7 min at 68 °C. Following temperature cycling, the reaction mixture was digested with 10 U DpnI to remove the methylated, non-mutated parental supercoiled dsDNA template. The mutated NS5B fragment was ligated into pFK I389 Lucubineo EI NS3-3'ET. To confirm the presence of the desired mutations, the entire NS5B insert was sequenced.

2.6. Transient transfection

Twenty micrograms of *in vitro* transcribed RNA was mixed with 400 μl of a suspension of 4×10^6 Huh-Lunet cells in a cuvette with a gap width of 0.4 cm (VWR International). After one pulse at 1600 V with an ECM 830 Electro Square Porator™ (BTX Harvard Apparatus), cells were immediately transferred into 20 ml of complete DMEM. One hundred microliters aliquots of the cell suspension were seeded in a 96-well plate (Falcon) previously filled with serial dilutions of the test inhibitors in complete DMEM. Cells were allowed to proliferate for 4 days at 37 °C, after which the luciferase activity was determined using the Steady-Glo luciferase assay system (Promega); the luciferase signal was measured using a Luminoskan Ascent (Thermo). The 50% effective concentration (EC_{50}) was defined as the concentration of inhibitor that reduced the luciferase signal by 50% when compared to non-treated transfected cells.

2.7. Replication fitness

Transfections were performed in Huh-Lunet cells as described above with the exception that cells were transfected with 5 μg RNA and 5 μg tRNA (Sigma Aldrich). Transfected cells were immediately transferred to 24 ml of complete DMEM and a 2 ml aliquot of the cell suspension was added to a 6-well plate (Iwaki). Cells were collected 4 h (normalization point), and 4 days after transfection to compare luciferase values with wild-type values, after extraction of the GND background signal. Cells transfected with the GND replicon [a replication-deficient subgenomic replicon encoding a GDD to GND mutation in NS5B (Targett-Adams and McLauchlan, 2005)] were used as a negative control reflecting background activity from the residual input RNA.

2.8. Clonal sequencing

The clonal sequence analysis protocol was adapted from Howe et al. (2008). Total cellular RNA from replicon-containing cells was extracted using the RNeasy minikit (Qiagen). In a two-step RT-PCR reaction, NS5B-containing cDNA was generated. The first strand cDNA was generated by reverse transcription (Transcriptor High Fidelity cDNA Synthesis Kit, Roche). Total cellular RNA (4 μg) was mixed gently with 1.2 nmol random hexamer primer, heated for 10 min at 65 °C to denature RNA secondary structures and placed on ice to allow the primer to anneal to the template RNA. Next, the RNA/primer mixture was added to 8.6 μl of reaction mix which contained 1× transcriptor high fidelity reverse transcriptase reaction buffer, 1 mM deoxynucleotide mix, 5 mM DTT, 20 U Protector RNase inhibitor and 10 U transcriptor high fidelity reverse transcriptase. Following incubation at 55 °C for 30 min, the RT reaction was terminated at 85 °C for 5 min. The NS5B gene was amplified using AccuPrime Pfx polymerase (Invitrogen). For this purpose, 10 μl of RT reaction was mixed with 30 pmol of primers 5919F and 7761R (5919F: 5′-GATCTAAGCGACGGGTCTT-3′; 7761R: 5′-CGTTCATCGGTTGGGGAGTA-3′), 1.25 U AccuPrime Pfx polymerase and 1× AccuPrime Pfx reaction mix (Howe et al., 2008). The PCR reaction was carried out at 95 °C for 2 min., followed by 25 cycles of (95 °C for 15 s; 60 °C for 30 s and 68 °C for 2 min.) The PCR products were evaluated by agarose gel electrophoresis. The 1.8 kb fragment was excised from the gel and purified by using a gel purification kit (Qiagen). The cDNA was ligated in the pJET1.2/blunt vector (Fermentas) and the resulting plasmid was transformed in One Shot chemical-competent *Escherichia coli* (TOP10 cells, Invitrogen). Colonies were randomly picked and plasmids containing the HCV NS5B insert were sequenced. Nucleotide sequences were determined by automated sequencing using BigDye terminator v. 3.1 (Applied Biosystems).

2.9. Molecular modeling

The modeling of the binding of JT-16 to the HCV NS5B polymerase was based on the HCV NS5B structure file 2BRK (with inhibitor CMF, 3-cyclohexyl-1-(2-morpholin-4-yl-2-oxoethyl)-2-phenyl-1H-indole-6-carboxylic acid, in the thumb domain 1) and was created by using Quatfit (CCL archives, http://www.ccl.net/) (Di Marco et al., 2005).

3. Results

3.1. HCV resistance selection with JT-16, a benzimidazole derivate

Resistance of HCV replicon to the benzimidazole inhibitor JT-16 (Fig. 1) was selected in a stepwise manner. Huh 9-13 replicon-con-

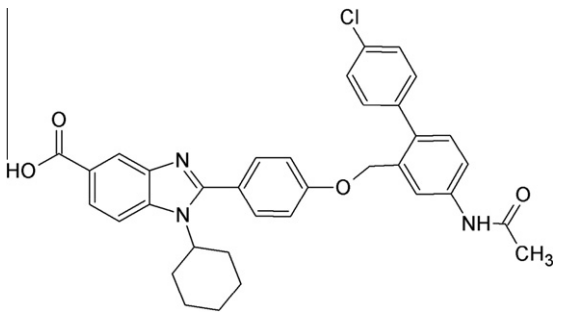

Fig. 1. Chemical structure of benzimidazole inhibitor JT-16.

taining cells were cultured in the presence of 1× EC_{50} of JT-16 for six passages. Following three passages at 1× EC_{50} of JT-16, the concentration of the inhibitor was doubled. This was repeated until the highest non-cytotoxic concentration was reached. The replicon-containing cells thus obtained were characterized by both genotypic (sequencing) and phenotypic (antiviral) assays. Phenotypic analysis revealed that the JT-16 resistant (JT-16res) replicon had a reduced susceptibility to JT-16 with a fold resistance value of ±12 (in comparison with wild-type (WT)) (Fig. 2).

The JT-16res replicon retained WT susceptibility to other non-nucleoside polymerase inhibitors that are known to target other regions of the polymerase (benzofuran HCV-796, thiophene carboxylic acid (TCA), benzothiadiazine GSK-4). Also nucleoside polymerase inhibitor 2′-C-methylcytidine (2′CMC) and protease inhibitor VX-950 retained their WT antiviral activity against the JT-16res replicon (Fig. 2).

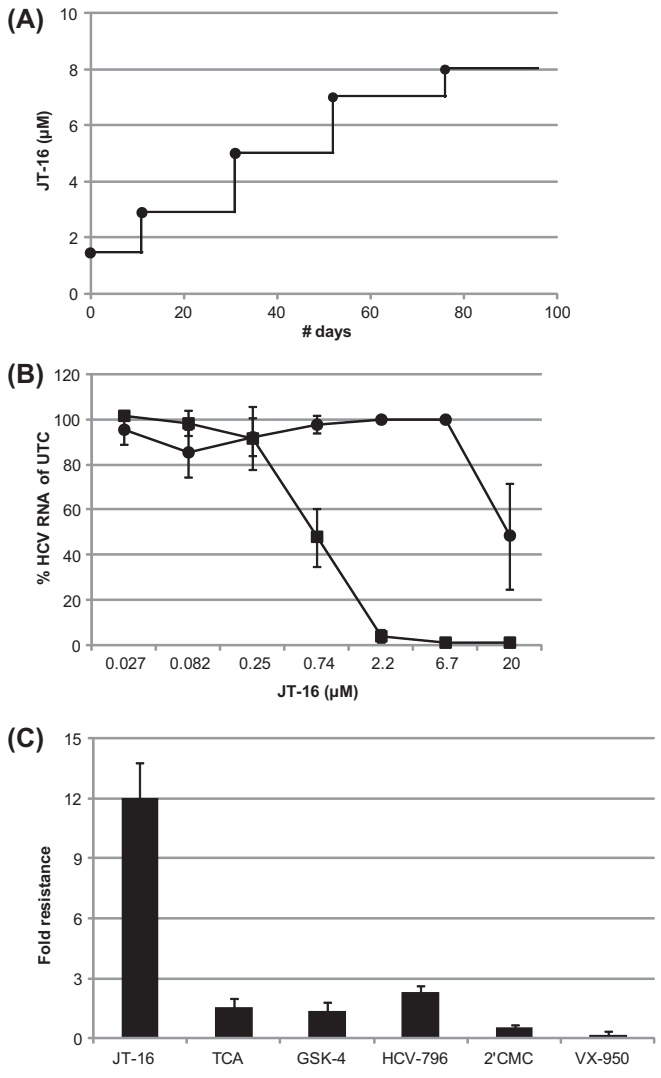

Fig. 2. Characterization of the phenotype of the JT-16res replicon. (A) JT-16 resistance selection. The graph depicts the number of days of passaging during the resistance selection in function of the concentrations of JT-16 that were used during each period. (B) Antiviral activity of JT-16 against wild-type (square) and JT-16res (circle) replicon-containing cells. Data shown are mean values ± SD of at least three independent experiments. (C) Fold resistance values of different HCV inhibitors in JT-16res replicon-containing cells. Fold resistance values are calculated as the ratio of the EC_{50} value in the JT-16res replicon to the EC_{50} value in wild-type replicon. Data shown are mean values ± SD for at least three independent experiments.

3.2. Genotypic characterization of JT-16 resistant replicon

The entire subgenomic region from JT-16res replicons was sequenced and compared to the sequence of WT Huh 9-13 replicons. Previously described resistance mutations for benzimidazole derivatives are located in the upper thumb domain of the HCV NS5B polymerase (P495A/L/S, P496S, and V499A) (Kukolj et al., 2005; Tomei et al., 2003). Genotypic characterization of the JT-16res replicon by population sequencing revealed the presence of mutation P495A, but only as a multispecies. In this JT-16res replicon a mutation at position T389 (T389S) was identified. Mutations at this position (T389A/S) were apparently also observed in double resistant replicons TCA+JT-16res and HCV-796+JT-16res (Delang et al., 2011b) and in a comparative study of resistance barriers with various HCV DAA (Directly Acting Antivirals) inhibitors (Delang et al., 2011a), suggesting that these mutations may be responsible for benzimidazole resistance. Clonal sequencing analysis of the JT-16res replicon revealed that the T389S mutation was present in 60% of all clones sequenced (n = 15), whereas the P495A mutation was identified in only 2 clones (=13%) (Fig. 3). Interestingly, these two mutations were never present together on the same genome. The C445F mutation emerged in 53% of the population and is probably a compensatory mutation. We previously showed that this mutation is not conferring resistance to JT-16 (fold resistance value: 1.1 ± 0.2, compared to WT) (Delang et al., 2011a).

To elucidate the role of mutation T389S and T389A in benzimidazole resistance, recombinant replicons with single variations (T389S, T389A, P495A, and P496S) were generated into a WT subgenomic luciferase replicon backbone by site-directed mutagenesis. Transient transfection assays were performed with these variants to determine their susceptibility to JT-16 and replication fitness. Mutants T389A and T389S exhibited a reduced susceptibility to JT-16 with fold resistance values of 7 and 13, respectively (Fig. 4). Mutation P495A had the most pronounced influence on the susceptibility to JT-16 with a fold resistance value of 44. On the contrary, P496S was found to be a low-level resistance mutation (3.4-fold). The P495A mutant also confers resistance to TCA, a thumb domain 2 inhibitor (16-fold). It was previously reported that a P495L mutant exhibits reduced susceptibility to thumb domain 2 inhibitors (Shi et al., 2008). The JT-16res mutants retained WT susceptibility to other HCV DAA inhibitors (VX-950, 2′CMC, TCA and HCV-796).

The replication fitness of each mutant was compared to that of WT replicon (Fig. 4). The replicative capacity of mutants T389S and P496S was slightly reduced when compared to WT (79% and 74%,

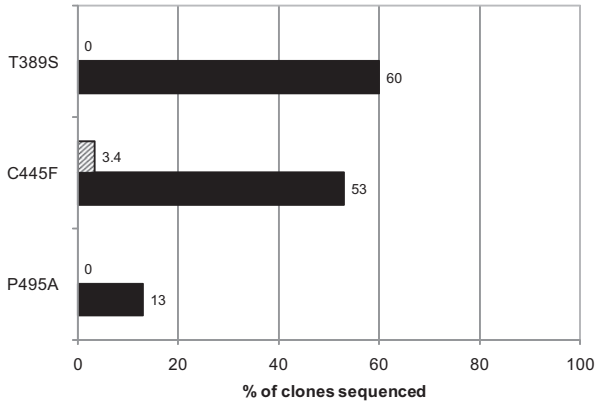

Fig. 3. Presence of JT-16 resistance or compensatory mutations in the JT-16res population determined by clonal sequencing. The graph depicts the percentage of clones carrying representative mutations identified in wild-type replicons (shaded) or in JT-16res replicons (black bars).

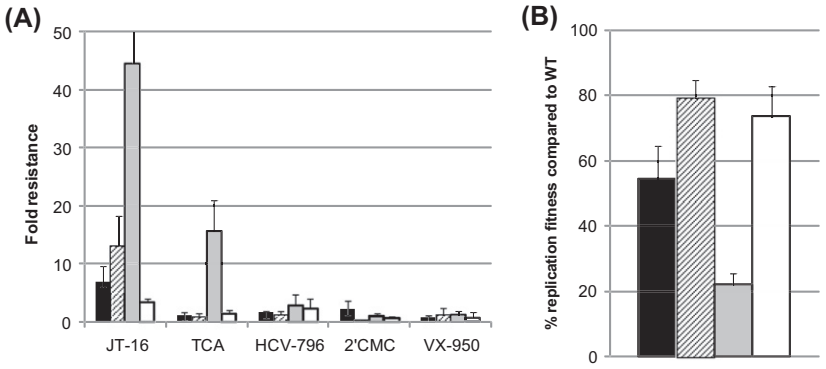

Fig. 4. Characterization of mutations conferring resistance to JT-16. T389A (black), T389S (shaded), P495A (light gray) and P496S (white). (A) Fold resistance values of several HCV inhibitors in Huh-Lunet cells transiently transfected with mutant replicon RNA. Inhibition of RNA replication by the selected inhibitors was measured by means of a luciferase assay at 72 h post transfection. Fold resistance values are calculated as the ratio of the EC_{50} value in mutant replicon to the EC_{50} value in wild-type replicon. Data shown are mean values ± SD of at least three independent experiments. (B) Replication fitness of the different JT-16res mutants. Huh-Lunet cells were transiently transfected with the mutant replicons. RNA replication was measured by means of a luciferase assay at 72 h post transfection. Data are normalized to the 4 h value post transfection to normalize for transfection efficiency. Values shown are expressed as a percentage of wild-type value at 72 h post transfection. Data are mean values ± SD for at least three independent experiments.

respectively). In contrast, replicons containing the P495A mutation had a markedly reduced replication fitness as compared to WT (22%). The replication fitness of T389A was decreased by approximately 50% when compared to WT. The difference in replicative capacity of replicons carrying mutations at position T389 or P495 may explain why mutations at T389 preferably emerged under JT-16 antiviral pressure instead of the previously described mutations at P495.

3.3. Three-dimensional model explaining the JT-16 resistant genotype

To explain the emergence of JT-16 resistance mutations at residue T389 in the thumb domain of HCV NS5B, JT-16 was superimposed onto the indole-based inhibitor CMF (3-cyclohexyl-1-(2-morpholin-4-yl-2-oxoethyl)-2-phenyl-1H-indole-6-carboxylic acid) from the 2BRK file using Quatfit (Di Marco et al., 2005). Although CMF is not a benzimidazole but an indole-based inhibitor, its structure resembles that of JT-16. Both structures differ by the position and nature of the side chain, which is positioned at the indole or phenyl group for CMF and JT-16, respectively. Crystallographic studies with CMF previously revealed that the cyclohexyl and phenyl ring substituents, bridged by an indole group, fill two closely spaced hydrophobic pockets. The side chains of L392, A395, T399, I424, H428 and F429 form a deep pocket, filled almost completely by the cyclohexyl group, whereas the V37 (finger domain), L392, A393, A396, L492 and V494 side chains form a narrower pocket that is occupied by the phenyl ring. One side of the indole core makes van der Waals interactions with the proline ring of P495 on the external lower side of the pocket. This interaction likely explains the observed resistance of P495 mutants to this class of inhibitors. In contrast to the CMF indole inhibitor, benzimidazole JT-16 has a long side chain at the para-position of the phenyl ring which extends into a hydrophobic cleft that is formed by, among other, K491 (Fig. 1). Amino acid T389 is located in close proximity to K491. Interestingly, whereas P495 is located at the surface of the thumb domain, T389 is facing the inside of the polymerase.

Although T389 is close to the binding site of JT-16, its side chain cannot be reached by the JT-16 inhibitor for hydrogen bonding interactions (Fig. 5). To clarify the potential role of T389 in JT-16 resistance, a ligplot interaction map of residue T389 was created. This interaction map reveals that T389 makes H-bonding interactions with C488, D387 and K491 (Fig. 6). Mutation of threonine 389 into an alanine or serine would disrupt this H-bonding network and may induce the change of rotameric state of the side chain of K491, thereby interfering with the binding of the JT-16 inhibitor.

4. Discussion

We report a novel resistance mutation for HCV benzimidazole inhibitors at residue T389 (T389A/S) in the HCV polymerase. These mutations emerged during *in vitro* resistance selection with benzimidazole JT-16 in genotype 1b subgenomic replicons. Phenotypic characterization of the JT-16res replicon revealed a reduced susceptibility to JT-16, whereas HCV inhibitors of other classes retained WT activity against this replicon. Sequence analysis revealed substitutions at NS5B residues T389, C445 and P495. To elucidate the role of these mutations in resistance to JT-16, variants were generated by introducing the mutations in a wild-type Con-1 scaffold. Mutants T389A and T389S resulted in moderate levels of resistance to JT-16 (7- and 13-fold, respectively), whereas P495A was associated with relatively high-level resistance (44-fold). Although the T389S mutant proved less resistant to JT-16 than the P495A mutant, T389S was identified as the dominant resistance mutation present in the JT-16res population (60% vs. 13%), as determined by clonal sequencing. Interestingly, these two mutations were never present together in the same genome. It is possible that the T389S mutation was preferred over the P495A mutation because of the higher replication fitness of the T389S mutant (79% vs. 22%). Since P495 is conserved in >99% of natural HCV isolates of all genotypes, a significant role for the region where P495 is located during HCV replication has been suggested, which may explain the lower replication efficiency of replicons in which its substitution was segregated.

In previously published resistance studies, replicons resistant to benzimidazole and indole derivatives have been isolated *in vitro* and were shown to carry mutations at residues P495, P496 or, to a lesser extent, V499 (Tomei et al., 2003; Kukolj et al., 2005). The T389A/S mutation was never described before to be involved in benzimidazole resistance. Interestingly, a mutation at the neighboring residue L392 (L392I) was earlier reported to reduce the susceptibility to NNIs binding to thumb domain 1 (Penuel et al., 2006). Furthermore, it was shown that a genotypic variant in genotype 2 at this position (L392I) resulted in a different shape of the binding pocket of thumb domain 1. Therefore, L392I is partly responsible for the resistance of the 2b polymerase to this class of inhibitors (Rydberg et al., 2009). Resistance selection with an indole-N-acet-

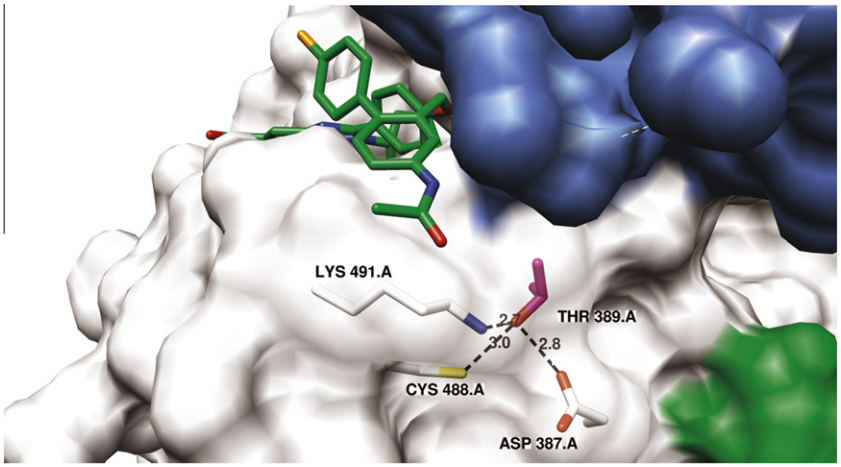

Fig. 5. JT-16 binding site in the thumb domain of the HCV polymerase. This figure was created using Chimera based on the superposition of the structure of the indole-based inhibitor CMF from the 2BRK file using Quatfit (Di Marco et al., 2005; Pettersen et al., 2004). Benzimidazole JT-16 is shown in green. Atom color coding: red, oxygen; blue, nitrogen; yellow, sulfur; gold, chlorine. Dashed black lines depict hydrogen-bonding interactions. (For interpretation of the references to color in this figure legend, the reader is referred to the web version of this article.)

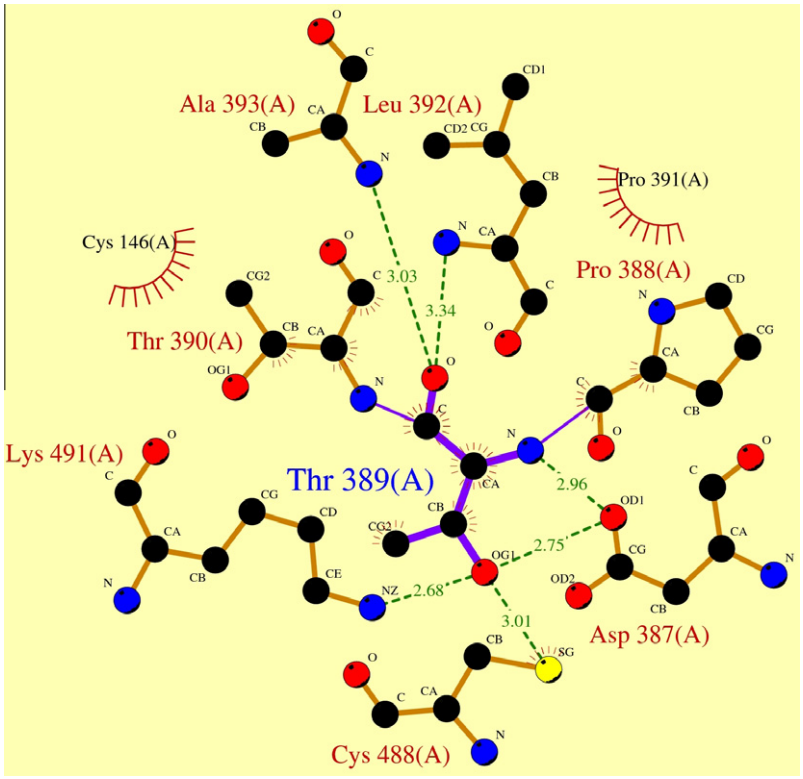

Fig. 6. Schematic representation of the interactions between residue T389 and neighboring residues. The interaction map of T389 was created by the program Ligplot (Wallace et al., 1995). Purple lines depict ligand bonds, brown lines non-ligand bonds. Dashed green lines represent H-bonding interactions and its length in Å. Non-ligand residues involved in hydrophobic contacts are represented by red semicircles. The corresponding atoms involved in hydrophobic contacts carry red spikes on the atom surface. Atom color coding: *red*, oxygen; *blue*, nitrogen; *yellow*, sulfur. (For interpretation of the references to color in this figure legend, the reader is referred to the web version of this article.)

amide resulted in about 30 drug resistant clones of which one clone harbored mutation L392I (Rydberg et al., 2009). The L392I mutation caused a narrowing of the binding pocket in proximity of the phenyl ring of the inhibitor.

That mutations at T389 were never described before as being involved in benzimidazole resistance, can probably be explained by the structural differences between the benzimidazole derivatives used in previous studies. For instance, the structure of a benzimidazole-5-carboxamide, 'compound C' in a study of Kukolj and colleagues, differs considerably from JT-16, with a furan ring instead of the phenyl ring attached to the benzimidazole moiety (Kukolj et al., 2005) (Fig. 7). Furthermore, 'compound C' has no extra substituents onto the furan ring, making this inhibitor shorter at the right-hand side of the molecule. In the supposition that it binds in a similar way as the indole inhibitor from the X-ray structure 2BRK, 'compound C' will be far away from residue T389 and its

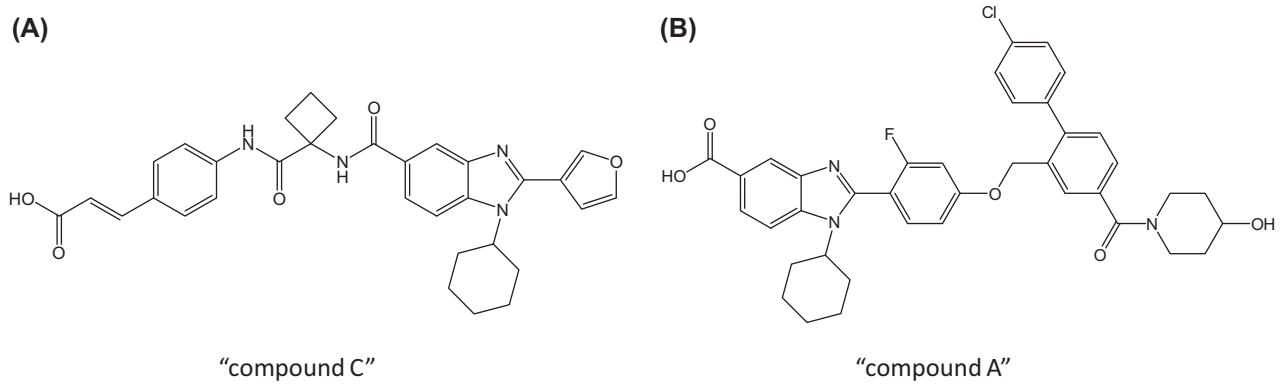

Fig. 7. Chemical structures of benzimidazole inhibitors previously used in *in vitro* resistance studies. A. 'compound C'(3-(4-(1-(1-cyclohexyl-2-(furan-3-yl)-1*H*-benzimidazole-5-carboxamido)cyclobutane carboxamido)phenyl)acrylic acid), (Kukolj et al., 2005); B. 'compound A' (2-[4-({4′-chloro-4-[4-hydroxypiperidin-1-yl)carbonyl]-1,1′-biphenyl-2-yl} methoxy)-2-fluorophenyl]-1-cyclohexyl-1*H*-benzimidazole-5-carboxylic acid), Tomei and colleagues (Tomei et al., 2003).

surroundings (Fig. 8). Hence, it is unlikely that a mutation at T389 would affect binding of 'compound C' to the HCV polymerase. Therefore, it seems logical that no mutations emerge at T389 under antiviral pressure of this inhibitor. On the contrary, the benzimidazole scaffold that is shared by both JT-16 and 'compound C' forms hydrophobic contacts with residues P495, V494, H428 and W500. These interactions explain likely the lack of inhibition of the P495A mutant by this class of DAAs. The low-level resistance of the P496S mutant for JT-16 can be explained by the lack of a side chain at the 5-carboxylate. In contrast, the potency of 'compound C', which has a carboxamide appendage at this position, was decreased by 10–25-fold by this mutation.

Tomei and colleagues reported an *in vitro* resistance study with a benzimidazole derivative that is structurally very similar to JT-16, 'compound A' (Fig. 7). Both inhibitors, JT-16 and compound A, have a similar side chain at the right-hand side of the molecule. Therefore, they probably bind to thumb domain 1 similarly, as shown in Fig. 8. However, because the part of 'compound A' that

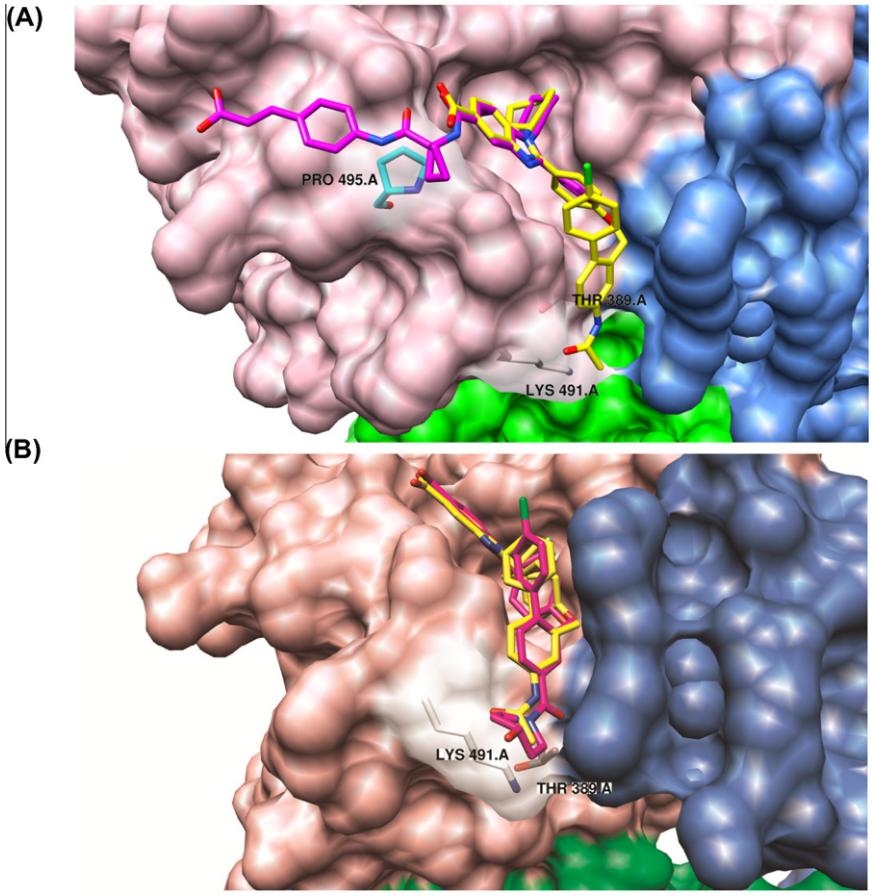

Fig. 8. Binding of JT-16 and previously reported benzimidazole derivatives to thumb domain I of the HCV polymerase (Kukolj et al., 2005; Tomei et al., 2003). A. JT-16 and 'compound C' from the study of Kukolj et al., (2005), B. JT-16 and 'compound A' from the study of Tomei et al., (2003). JT-16 is shown in yellow; the other benzimidazoles are shown in purple. The thumb, palm and finger domain of HCV polymerase are shown in pink, green and blue, respectively. (For interpretation of the references to color in this figure legend, the reader is referred to the web version of this article.)

interacts with K491 may be larger than that of the JT-16 inhibitor (4′-hydroxypiperidine vs. acetamide), the favorable interaction with K491 (a hydrophobic interaction between the piperidine ring and the K491 side chain) is more important than a possible steric hindrance between this inhibitor and K491 if this residue would adopt another rotamer. Hence, there would probably be no effect on the binding of this inhibitor to the thumb domain 1 when T389 is mutated. It has been reported that K491 faces the active site within the palm domain and that it interacts with residues in the Δ1-fingerloop (Deval et al., 2007). When the lysine at this position was mutated to glutamic acid, the enzymatic activity of the NS5B was significantly reduced. Therefore, it is possible that mutants at this position are not able to replicate.

Because of the high genetic variability of the HCV population in infected patients and the error rate of the HCV polymerase, it is unlikely that benzimidazole inhibitors or other HCV DAAs will be used successfully in mono-therapy. In particular non-nucleoside polymerase inhibitors are considered as antivirals with a low barrier to resistance. The resistance barrier is affected by (i) the genetic barrier to resistance, which is defined as the sum of mutations needed to acquire full resistance, (ii) the *in vivo* fitness of the viral variant, and (iii) the drug exposure, defined as the drug concentration achieved in the treated patient (Pawlotsky, 2011). It is possible that a less resistant, but fitter, virus is clinically more significant than a highly resistant, but poorly fit variant. As a single substitution (T389S or P495A) is sufficient to confer moderate to high levels of resistance to JT-16, the genetic barrier to resistance of JT-16 is rather low, as for other NNIs in development. Few *in vivo* resistance data have been reported with NNIs targeting thumb domain 1 administered as mono-therapy. Sequence analysis at day 5 of BILB 1941 mono-therapy failed to detect the selection of any sequence changes that were consistent with known resistant mutants. However, baseline NS5B variants were found that exhibited either enhanced or reduced susceptibility to inhibition by BILB1941. Among these, NS5B substitutions of amino acids (V494I or I424V, V494A, P496A) in thumb pocket 1 were identified (Marquis et al., 2008). BI 207127 resistant mutants that encode P495 substitutions were observed in 11% of patients who received 5-day mono-therapy. Follow-up to BI 207127 treatment revealed that the wild-type sequences re-emerged rapidly from day 6 to 14 (Lagace et al., 2010).

In conclusion, we demonstrate that less resistant but fitter HCV genotype 1b variants can develop during *in vitro* resistance selection with benzimidazole JT-16. Mutations at amino acid T389 confer moderate levels of resistance to JT-16. Surprisingly, the previously published 'key' mutation for benzimidazole resistance, P495A, was detected in only 13% of the resistant population. Our data show that structural modifications to inhibitors with a similar scaffold can affect the resistance mutations that emerge during resistance selection and thus that drug resistant mutants should not be largely ascribed to a family of compounds but should be defined for different analogs within a given family.

Acknowledgements

This work was supported by a fellowship to Leen Delang from the Research Foundation Flanders (FWO) and grant G.0728.09N from the FWO.

References

Beaulieu, P.L., Gillard, J., Bykowski, D., Brochu, C., Dansereau, N., Duceppe, J.S., Hache, B., Jakalian, A., Lagace, L., LaPlante, S., McKercher, G., Moreau, E., Perreault, S., Stammers, T., Thauvette, L., Warrington, J., Kukolj, G., 2006. Improved replicon cellular activity of non-nucleoside allosteric inhibitors of HCV NS5B polymerase: from benzimidazole to indole scaffolds. Bioorg. Med. Chem. Lett. 16, 4987–4993.

Brainard, D.M., Anderson, M.S., Petry, A., Van Dyck, K., De Lepeleire, I., Sneddon, K., Cummings, C.E., Nachbar, R.B., Barnard, R.J., Sun, P., Panorchan, P., Sanderson, J.B., Udezue, E., Wagner, F., Iwamoto, M., Chodakewitz, J., Wagner, J.A., 2009. Safety and antiviral activity of NS5B polymerase inhibitor MK-3281, in treatment-naïve genotype 1a, 1b and 3 HCV-infected patients. Hepatology 50, 1026A–1027A.

Bressanelli, S., Tomei, L., Rey, F.A., De Francesco, R., 2002. Structural analysis of the hepatitis C virus RNA polymerase in complex with ribonucleotides. J. Virol. 76, 3482–3492.

Bressanelli, S., Tomei, L., Roussel, A., Incitti, I., Vitale, R.L., Mathieu, M., De Francesco, R., Rey, F.A., 1999. Crystal structure of the RNA-dependent RNA polymerase of hepatitis C virus. Proc. Natl. Acad. Sci. USA 96, 13034–13039.

Delang, L., Coelmont, L., Neyts, J., 2010. Antiviral therapy for hepatitis C virus: beyond the standard of care. Viruses 2, 826–866.

Delang, L., Paeshuyse, J., Vliegen, I., Leyssen, P., Obeid, S., Durantel, D., Zoulim, F., Op De Beeck, A., Neyts, J., 2009. Statins potentiate the in vitro anti-hepatitis C virus activity of selective hepatitis C virus inhibitors and delay or prevent resistance development. Hepatology 50, 6–16.

Delang, L., Vliegen, I., Froeyen, M., Neyts, J., 2011a. Comparative study of the genetic barrier and pathways towards resistance of selective inhibitors of HCV replication. Antimicrob. Agents Chemother. 55, 4103–4113.

Delang, L., Vliegen, I., Leyssen, P., Neyts, J., 2011b. In vitro selection and characterization of HCV replicons resistant to multiple non-nucleoside polymerase inhibitors. J. Hepatol, in press.

Deval, J., D'Abramo, C.M., Zhao, Z., McCormick, S., Coutsinos, D., Hess, S., Kvaratskhelia, M., Gotte, M., 2007. High resolution footprinting of the hepatitis C virus polymerase NS5B in complex with RNA. J. Biol. Chem. 282, 16907–16916.

Di Marco, S., Volpari, C., Tomei, L., Altamura, S., Harper, S., Narjes, F., Koch, U., Rowley, M., De Francesco, R., Migliaccio, G., Carfi, A., 2005. Interdomain communication in hepatitis C virus polymerase abolished by small molecule inhibitors bound to a novel allosteric site. J. Biol. Chem. 280, 29765–29770.

Erhardt, A., Deterding, K., Benhamou, Y., Reiser, M., Forns, X., Pol, S., Calleja, J.L., Ross, S., Spangenberg, H.C., Garcia-Samaniego, J., Fuchs, M., Enriquez, J., Wiegand, J., Stern, J., Wu, K., Kukolj, G., Marquis, M., Beaulieu, P., Nehmiz, G., Steffgen, J., 2009. Safety, pharmacokinetics and antiviral effect of BILB 1941, a novel hepatitis C virus RNA polymerase inhibitor, after 5 days oral treatment. Antiviral Ther. 14, 23–32.

Friebe, P., Boudet, J., Simorre, J.P., Bartenschlager, R., 2005. Kissing-loop interaction in the 3′ end of the hepatitis C virus genome essential for RNA replication. J. Virol. 79, 380–392.

Hashimoto, H., 2005. Fused cyclic compounds and medicinal use thereof. Patent EP02743728 EP(WO2003000254 A1).

Herlihy, K.J., Graham, J.P., Kumpf, R., Patick, A.K., Duggal, R., Shi, S.T., 2008. Development of intergenotypic chimeric replicons to determine the broad-spectrum antiviral activities of hepatitis C virus polymerase inhibitors. Antimicrob. Agents Chemother. 52, 3523–3531.

Hong, Z., Cameron, C.E., Walker, M.P., Castro, C., Yao, N.H., Lau, J.Y.N., Zhong, W.D., 2001. A novel mechanism to ensure terminal initiation by hepatitis C virus NS5B polymerase. Virology 285, 6–11.

Howe, A.Y., Cheng, H., Johann, S., Mullen, S., Chunduru, S.K., Young, D.C., Bard, J., Chopra, R., Krishnamurthy, G., Mansour, T., O'Connell, J., 2008. Molecular mechanism of hepatitis C virus replicon variants with reduced susceptibility to a benzofuran inhibitor, HCV-796. Antimicrob. Agents Chemother. 52, 3327–3338.

Kukolj, G., McGibbon, G.A., McKercher, G., Marquis, M., Lefebvre, S., Thauvette, L., Gauthier, J., Goulet, S., Poupart, M.A., Beaulieu, P.L., 2005. Binding site characterization and resistance to a class of non-nucleoside inhibitors of the hepatitis C virus NS5B polymerase. J. Biol. Chem. 280, 39260–39267.

Lagace, L., Cartier, M., Laflamme, G., Lawetz, C., Marquis, M., Triki, I., Bernard, M.J., Bethell, R., Larrey, D.G., Lueth, S., Trepo, C., Stern, J.O., Boecher, W.O., Steffgen, J., Kukolj, G., 2010. Genotypic and phenotypic analysis of the NS5B polymerase region from viral isolates of HCV chronically infected patients treated with BI 207127 for 5-days monotherapy. Hepatology 52, 1205A.

LaPlante, S.R., Jakalian, A., Aubry, N., Bousquet, Y., Ferland, J.M., Gillard, J., Lefebvre, S., Poirier, M., Tsantrizos, Y.S., Kukolj, G., Beaulieu, P.L., 2004. Binding mode determination of benzimidazole inhibitors of the hepatitis C virus RNA polymerase by a structure and dynamics strategy. Angew. Chem. Int. Ed Engl. 43, 4306–4311.

Larrey, D.G., Benhamou, Y., Lohse, A.W., Trepo, C., Moelleken, C., Bronowicki, J.P., Heim, M.H., Arasteh, K., Zarski, J.P., Bourliere, M., Wiest, R., Calleja, J.L., Enriquez, J., Erhardt, A., Wedemeyer, H., Gerlach, T., Berg, T., Stern, J.O., Wu, K., Abdallah, N., Nehmiz, G., Boecher, W.O., Berger, F.M., Steffgen, J., 2009. Bi 207127 is a potent Hcv RNA polymerase inhibitor during 5 days monotherapy in patients with chronic hepatitis C. Hepatology 50, 1044A.

Leveque, V.J.P., Johnson, R.B., Parsons, S., Ren, J.X., Xie, C.P., Zhang, F.M., Wang, Q.M., 2003. Identification of a C-terminal regulatory motif in hepatitis C virus RNA-dependent RNA polymerase: structural and biochemical analysis. J. Virol. 77, 9020–9028.

Lohmann, V., Korner, F., Koch, J., Herian, U., Theilmann, L., Bartenschlager, R., 1999. Replication of subgenomic hepatitis C virus RNAs in a hepatoma cell line. Science 285, 110–113.

Marquis, M., Deterding, K., Erhardt, A., Benhamou, Y., Moelleken, C., Forns, X., Pol, S., Calleja, J.L., Ross, S., Spangenberg, H.C., Torro, C., Fuchs, M., Enriquez, J., Wiegand, J., Beaulieu, P., Nehmiz, G., Steffgen, J., Stern, J.O., Kukolj, G., 2008.

Genotypic and phenotypic analysis of hepatitis C virus NS5B polymerase variants to BILB1941 inhibition. Hepatology 48, 1159A.
Paeshuyse, J., Vliegen, I., Coelmont, L., Leyssen, P., Tabarrini, O., Herdewijn, P., Mittendorfer, H., Easmon, J., Cecchetti, V., Bartenschlager, R., Puerstinger, G., Neyts, J., 2008. Comparative in vitro anti-hepatitis C virus activities of a selected series of polymerase, protease, and helicase inhibitors. Antimicrob. Agents Chemother. 52, 3433–3437.
Pawlotsky, J.M., 2011. Treatment failure and resistance with direct acting antiviral drugs against hepatitis C virus. Hepatology 53, 1742–1751.
Penuel, E., Han, D., Favero, K., Lam, E., Liu, Y., Parkin, N.T., 2006. Variable non-nucleoside inhibitor susceptibility among untreated HCV-infected patient samples. 1st International Workshop on Hepatitis C: Resistance and New Compounds. Abstract 18.
Pettersen, E.F., Goddard, T.D., Huang, C.C., Couch, G.S., Greenblatt, D.M., Meng, E.C., Ferrin, T.E., 2004. UCSF chimera – A visualization system for exploratory research and analysis. J. Comput. Chem. 25, 1605–1612.
Rydberg, E.H., Cellucci, A., Bartholomew, L., Mattu, M., Barbato, G., Ludmerer, S.W., Graham, D.J., Altamura, S., Paonessa, G., De Francesco, R., Migliaccio, G., Carfi, A., 2009. Structural basis for resistance of the genotype 2b hepatitis C virus NS5B polymerase to site A non-nucleoside inhibitors. J. Mol. Biol. 390, 1048–1059.
Shepard, C.W., Finelli, L., Alter, M.J., 2005. Global epidemiology of hepatitis C virus infection. Lancet Infect. Dis. 5, 558–567.
Shi, S.T., Herlihy, K.J., Graham, J.P., Fuhrman, S.A., Doan, C., Parge, H., Hickey, M., Gao, J., Yu, X., Chau, F., Gonzalez, J., Li, H., Lewis, C., Patick, A.K., Duggal, R., 2008. In vitro resistance study of AG-021541, a novel nonnucleoside inhibitor of the hepatitis C virus RNA-dependent RNA polymerase. Antimicrob. Agents Chemother. 52, 675–683.
Targett-Adams, P., McLauchlan, J., 2005. Development and characterization of a transient-replication assay for the genotype 2a hepatitis C virus subgenomic replicon. J. Gen. Virol. 86, 3075–3080.
Tomei, L., Altamura, S., Bartholomew, L., Biroccio, A., Ceccacci, A., Pacini, L., Narjes, F., Gennari, N., Bisbocci, M., Incitti, I., Orsatti, L., Harper, S., Stansfield, I., Rowley, M., De Francesco, R., Migliaccio, G., 2003. Mechanism of action and antiviral activity of benzimidazole-based allosteric inhibitors of the hepatitis C virus RNA-dependent RNA polymerase. J. Virol. 77, 13225–13231.
Wallace, A.C., Laskowski, R.A., Thornton, J.M., 1995. LIGPLOT: a program to generate schematic diagrams of protein–ligand interactions. Protein Eng. 8, 127–134.
Zeuzem, S., Berg, T., Moeller, B., Hinrichsen, H., Mauss, S., Wedemeyer, H., Sarrazin, C., Hueppe, D., Zehnter, E., Manns, M.P., 2009. Expert opinion on the treatment of patients with chronic hepatitis C. J. Viral Hep. 16, 75–90.